ACS APPLIED MATERIALS & INTERFACES

Research Article

www.acsami.org

Solution-Grown Germanium Nanowire Anodes for Lithium-Ion Batteries

Aaron M. Chockla, Kyle C. Klavetter, C. Buddie Mullins, and Brian A. Korgel*

Department of Chemical Engineering, Texas Materials Institute, Center for Nano- and Molecular Science and Technology, The University of Texas at Austin, Austin, Texas 78712-1062, United States

ABSTRACT: Solution-grown germanium (Ge) nanowires were tested as high capacity anodes in lithium ion (Li-ion) batteries. Nanowire films were formulated and cast as slurries with conductive carbon (7:1 Ge:C w/w), PVdF binder and 1.0 M $LiPF_6$ dissolved in various solvents as electrolyte. The addition of fluorethylene carbonate (FEC) to the electrolyte was critical to achieving stable battery cycling and reversible capacities as high as 1248 mA h g^{-1} after 100 cycles, which is close to the theoretical capacity of 1,384 mA h g^{-1}. Ge nanowire anodes also exhibited high rate capability, with reversible cycling above 600 mA h g^{-1} for 1200 cycles at a rate of 1C. The batteries could also be discharged at 10C with a capacity of 900 mA h g^{-1} when charged at 1C.

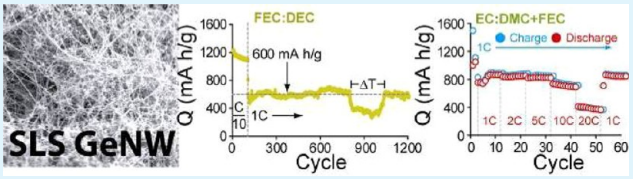

KEYWORDS: *energy storage, lithium-ion battery, germanium nanowires, electrochemistry, anode*

INTRODUCTION

Lithium-ion (Li-ion) batteries are used to power portable electronic devices because of their relatively high charge storage capacity, high energy density, slow self-discharge and lack of memory effect.[1−3] Still, lower cost, lighter weight and smaller volume Li-ion batteries are greatly desired. New application in electric powered vehicles and for large-scale energy storage require batteries with unprecedented energy and power density.[2] The only way to achieve this is to use different electrode materials with higher charge storage capacity.[2−4]

Li-ion batteries consist of a cathode that is a Li metal oxide compound (largely $LiCoO_2$) and a graphite anode.[2,3] On the anode side, graphite has a maximum Li storage capacity of 372 mA h g^{-1}. Several materials have significantly higher Li storage capacity, including silicon (Si) and germanium (Ge).[3,4] Si has received significant attention because it has the highest possible gravimetric Li storage capacity of any known material of 3,579 mA h g^{-1}.[5] Si is also an abundant natural resource and relatively inexpensive. Ge is significantly more expensive than Si, but is nonetheless worth considering as a replacement for graphite for some applications, particularly those that require high power density. Ge has a lower maximum capacity than Si, of 1,384 mA h g^{-1}, but it is still much higher than graphite,[5] and given the current capacity limits of the cathode, either Si or Ge would increase the total battery capacity by about 25% as shown in Figure 1. Si and Ge also have similar volumetric capacity, 7366 A h L^{-1} for Ge (based on $Li_{15}Ge_4$) and 8,334 A h L^{-1} for Si (based on $Li_{15}Si_4$).[5] Ge also has significant advantages over Si. It is more electrically conductive because of its lower band gap, providing for more efficient charge injection, especially in thicker anodes. Perhaps most significantly, Li diffusion is 400 times faster in Ge than in Si,[6] which gives Ge a much higher rate capability than Si (and graphite), which is extremely important in applications needing significantly higher power density like electric vehicle applications that require very high discharge power.[7,8] There is also evidence that Ge anodes are more stable than Si anodes: Si and Ge both expand considerably upon lithiation (280% for Si and 240% for Ge), but the lithiation pathways are different, with Si lithiation being highly anisotropic and Ge lithiation occurring isotropically.[5]

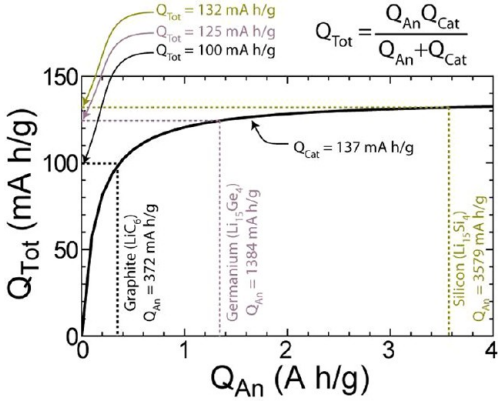

Figure 1. Total charge capacity Q_{tot}, of a Li-ion battery depends on the capacities of both the cathode and anode, Q_{cat} and Q_{an}. With the current cathode ($LiCoO_2$) capacity of about 137 mA h g^{-1}, replacing graphite with either Ge or Si would increase Li-ion battery capacity by about 25%.

Ge thin films.[7,9−15] nanoparticles,[15−17] nanowires,[18−22] and nanotubes,[8] have been studied as anodes in Li-ion batteries with good results. Here, we study reasonably thick (>10 μm) Ge nanowire anodes processed from slurries. The studies are enabled by the synthesis of large amounts of Ge nanowires using

Received: June 6, 2012
Accepted: August 15, 2012
Published: August 15, 2012

   dx.doi.org/10.1021/am3010253 | *ACS Appl. Mater. Interfaces* 2012, 4, 4658−4664

a colloidal solution-phase process.[23] Poly(vinylidene fluoride) (PVdF) was used as binder and several electrolyte solvents were studied. The addition of fluoroethylene carbonate (FEC) to the electrolyte was found to provide a significant stabilizing effect on the battery performance. A reversible capacity of 1248 mA h g^{-1}, close to the theoretical capacity of Ge, was observed after 100 cycles. Charging at a relatively fast cycle rate of 1C and discharging at a very fast rate of 10*C* gave capacities of 900 mA h g^{-1}.

MATERIALS AND METHODS

Materials. All reagents and solvents were used as received without further purification. Dodecanethiol (DDT, ≥98%), tetrachloroaurate trihydrate (≥99.9%), sodium borohydride (≥98%), toluene (anhydrous, 99.8%), ethanol (99.9%), tetraoctylammonium bromide (TOAB, 98%), propylene carbonate (PC, anhydrous, 99.7%), lithium hexafluorophosphate ($LiPF_6$, ≥99.99%), poly (vinylidene fluoride) (PVdF, avg MW ~534,000 by GPC), 1-methyl 2-pyrrolidinone (NMP, 99.5%), chloroform (99.8%) and squalane (99%) were purchased from Sigma-Aldrich and diphenyl germane (DPG, >95%) from Gelest. Dimethyl carbonate (DMC, ≥99%, anhydrous) and diethyl carbonate (DEC, ≥99%, anhydrous) were purchased from Sigma. Conductive carbon super C65 was supplied by TIMCAL. Fluoroethylene carbonate (FEC, >98%) was supplied by TCI America. Ethylene carbon (EC) based electrolyte EC:DEC was purchased from Novolyte and EC:DMC was obtained from EMD Chemicals. Celgard 2400 membranes (25μm) were provided by Celgard. Li metal foil (1.5 mm 99.9%) was purchased from Alfa Aesar. Dodecanethiol-coated Au nanocrystals (2 nm diameter) were synthesized following literature procedures[24] and stored in a nitrogen-filled gloved box as a stock dispersion in toluene at a concentration of 50 mg mL^{-1}.

Ge Nanowire Synthesis. Ge nanowires were produced by solution-liquid-solid (SLS) growth using Au nanocrystal seeds and DPG reactant.[23] In a typical reaction, 10 mL of squalane is added to a 4-neck flask, attached to a Schlenk line and heated to 100°C with vigorous stirring under vacuum (<500 mTorr) for 30 min, and then blanketed with nitrogen. A DPG reactant solution is prepared in a nitrogen-filled glove box by combining 0.275 mL of the Au nanocrystal stock solution with 0.375 mL of DPG and 1 mL of squalane. The reactant solution is removed from the glovebox in a syringe and rapidly injected into the reaction flask containing the hot squalane. After 5 min, the flask is removed from the heating mantle and allowed to cool to room temperature. The reaction mixture is transferred to a centrifuge tube with an additional 10 mL of toluene. The nanowires are precipitated by centrifugation at 8000 rpm for 5 minutes. The supernatant is discarded. The nanowires are redispersed in a mixture of chloroform and ethanol and reprecipitated by centrifugation twice more to remove residual reactant byproducts and squalane. About 40−50 mg of Ge nanowires are obtained from a single reaction.

Ge Nanowire Anode Preparation and Battery Assembly. Slurries of 70:20:10 w/w/w Ge nanowires:PVdF:carbon were used in the battery tests. In a typical preparation, Ge nanowires (81.1 mg) are dispersed in 2 mL toluene with 1 h of bath sonication. 23.2 mg PVdF and 11.6 mg conductive carbon are dissolved in 1 mL NMP with 1 h of bath sonication. The Ge nanowire and PVdF/carbon black suspensions are mixed and wand sonicated for 30 minutes and then the volume is reduced on a rotary evaporator to form a thick slurry. The slurry is doctor-bladed (200 μm gap) onto Cu foil and vacuum dried overnight at 100°C. Individual 11 mm diameter circular electrodes are hole-punched from the coated Cu foil. Typical mass loading is 1 mg cm^{-2}.

The Ge-coated Cu films are brought into an Ar-filled glovebox (<0.1 ppm O_2) for coin cell assembly. 2032 stainless steel coin cells are used with Li foil as the counter electrode. The battery is assembled from the Li counter electrode by placing a few drops of electrolyte, followed by the Celgard 2400 separator membrane (25μm thick, Celgard), another few drops of electrolyte, and then the Ge electrode. The battery is crimped and removed from the glovebox for testing.

Material Characterization. Scanning electron microscopy (SEM) images were acquired using a Zeiss Supra 40 SEM with an in-lens arrangement, a working voltage of 5 keV and a working distance of 5 mm. SEM samples were imaged silicon wafers (S.E.H). Transmission electron microscopy (TEM) images were digitally acquired using either a FEI Tecnai Spirit BioTwin TEM operated at 80 kV or a field emission JEOL 2010F TEM operated at 200 kV. TEM samples were prepared by drop-casting from chloroform dispersions onto 200 mesh lacey-carbon copper TEM grids (Electron Microscopy Sciences).

X-ray diffraction (XRD) was performed on a Rigaku R-Axis Spider Diffractometer with Image plate detector with Cu-k_α (λ = 1.5418 Å) radiation operated at 40 kV and 40 mA. Measurements using were taken with samples on a 0.5 mm nylon loop. Samples were scanned for 10 min while rotating at 1° per s under ambient conditions. Diffraction data were integrated with subtraction of the background scattering from the nylon loop.

Galvanostatic measurements were made using an Arbin BT-2143 test unit with cycling between 0.01 and 2 V vs Li/Li^+. Capacities are reported based on active material only and rates are reported based on the theoretical capacity of Ge, i.e., 1*C* = 1384 mA g^{-1}. The terms charge and discharge are used as they would be in a full cell with a metal oxide cathode and refer to lithiation and delithiation, respectively.

RESULTS AND DISCUSSION

Ge Nanowires. Figure 2 shows SEM and TEM images and XRD data of the Ge nanowires used for the Li-ion battery studies.

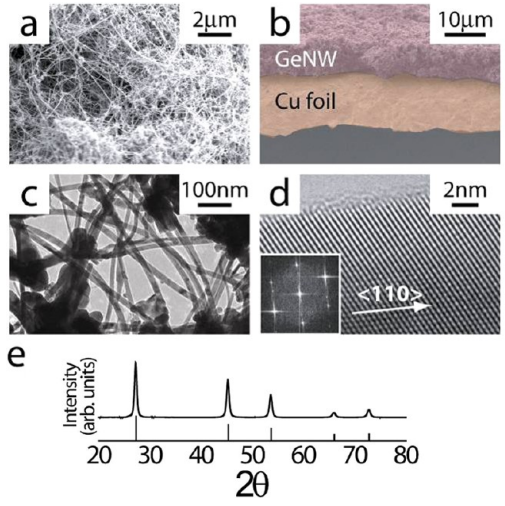

Figure 2. (a) SEM image of SLS-grown Ge nanowires. (b) SEM image of a cross-sectioned Ge nanowire anode. (c, d) TEM images of Ge nanowires; the inset in d is the FFT of the TEM image used to determine the ⟨110⟩ growth direction of the nanowire. (e) XRD of Ge nanowires with the reference pattern provided for diamond cubic Ge (JCPDS: 00-004-0545).

The nanowires were made by the Au nanocrystal-seeded SLS process[23] and are crystalline, diamond cubic Ge, with an average diameter of 30 nm and lengths of tens of micrometers. The nanowires were formulated into slurries and deposited as relatively thick (10 μm) anode films with loadings of about 1 mg cm^{-2}. There have been only a few studies of thick-film anodes of Si[25−27] and Ge[18] nanowires (and Ge nanotubes[8]). The quantity of Au used in the synthesis is relatively low (1250:1 Ge:Au) and it does not appear in the XRD pattern.

Ge Nanowire Li-Ion Battery Performance. Li-ion batteries with Ge nanowire anodes were tested using PVdF binder, conductive carbon (7:1 w/w Ge:C) and 1.0 M $LiPF_6$ electrolyte in various mixtures of the carbonates. Figure 3 shows the charge capacity and capacity retention of batteries cycled between 0.01 and 2 V vs Li/Li^+ at a rate of C/10 (*C* = 1384 mA h g^{-1}) and the battery results are also tabulated in Table 1. The addition of FEC

dx.doi.org/10.1021/am3010253 | ACS Appl. Mater. Interfaces 2012, 4, 4658−4664

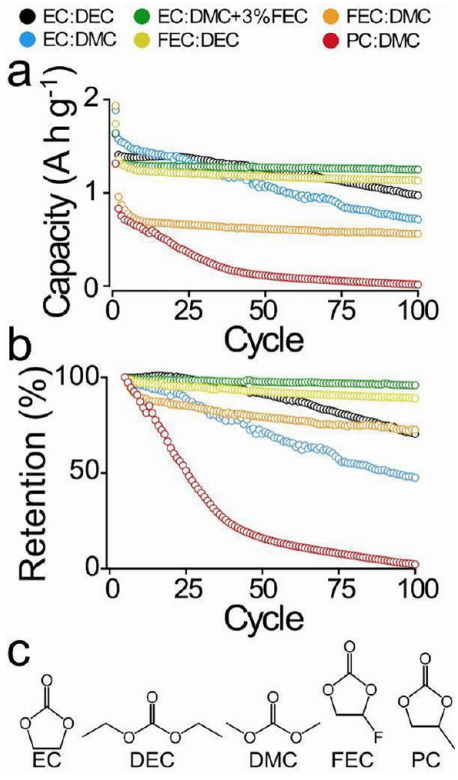

Figure 3. (a) Charge (lithiation) capacity and (b) capacity retention (relative to the 5th cycle) for Ge nanowire anodes (7:1:2 w/w/w Ge:C:PVdF) with 1.0 M $LiPF_6$ electrolyte in various solvents. (c) Molecular representations of the electrolytes studied. The cycle rate was $C/10$.

Table 1. Summary of Ge Nanowire Anode Battery Performance

	capacity (mA h g^{-1})				retention (%)	
electrolyte	cycle 1	1st cycle loss (%)	cycle 5	cycle 100	Q_{ret1} [a]	Q_{ret5} [b]
EC:DEC	1630	223 (13.7)	1382	973	59.7	70.4
EC:DMC	1885	311 (16.5)	1504	714	37.9	47.5
EC:DMC +FEC	1639	301 (18.4)	1303	1248	76.1	95.8
FEC:DEC	1738	385 (22.2)	1271	1131	65.0	89.0
FEC:DMC	1933	975 (50.5)	774	561	29.0	72.5
PC:DMC	1313	484 (36.8)	699	15	1.2	2.2

[a]Charge capacity retention of the 100th cycle relative to the 1st cycle [b]Charge capacity retention of the 100th cycle relative to the 5th cycle

to the electrolyte was of particular interest because studies have shown that FEC helps stabilize battery performance in Si-based anodes.[28−31] In the Ge nanowire anodes, FEC addition was also found to provide a stabilizing effect for the Ge nanowire batteries and EC:DMC+3%FEC electrolyte yielded capacity of 1248 mA h g^{-1} after 100 cycles, corresponding to only a 4.2% loss in capacity relative to the 5th cycle. These values are higher than recent reports for Ge nanowires used as Li-ion battery negative electrodes. For example, Seo et al. recently reported capacities of ∼700 mA h g^{-1} for SLS-grown Ge nanowires after 100 cycles using a current density of 400 mA g^{-1} (∼$C/3$).[18] Chan et al. reported capacities of 1000 mA h g^{-1} after 20 cycles at a current load of 80 mA h g^{-1} (rate of $C/20$) for Ge nanowires grown directly from steel substrates using a CVD process.[21] Electrolytes with DEC outperformed those with DMC and PC:DMC had the worst performance.

PVdF appears to be much more effective as a binder for Ge than Si. Recently, PVdF was found to be a poor binder for Si nanowire anodes,[25] but the performance here for Ge nanowires with PVdF is very good. PVdF has achieved some good results with Si particles, but only with high temperature (300°C) annealing to improve the interfacial chemistry and a help distribute the binder and conductive carbon throughout the active material,[32,33] and several other binders like sodium alginate have been shown to work better much better for Si.[34−37] Ge on the other hand appears to interface well with PVdF.

Voltage Profiles and Differential Capacity Plots. Figure 4 shows charge and discharge capacities, Coulombic efficiency

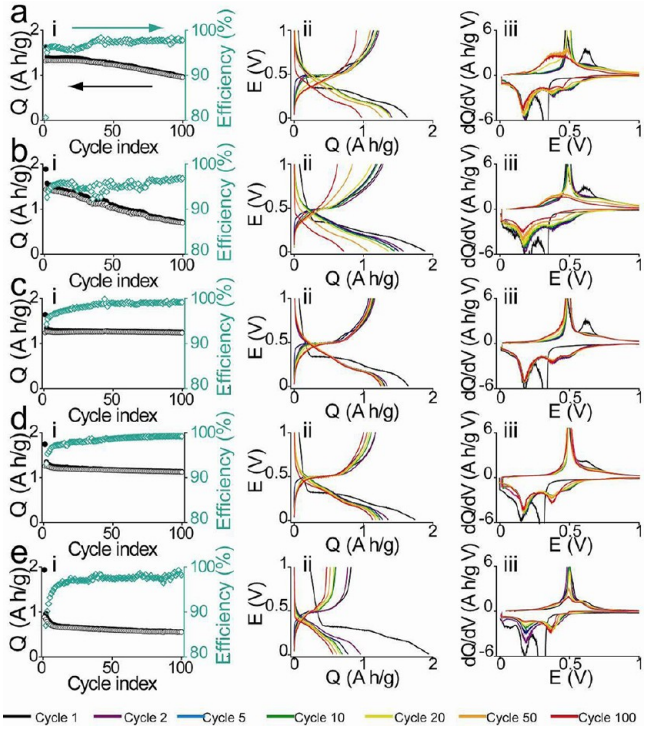

Figure 4. (i) Charge (lithiation) and discharge (delithiation) capacities plotted with coulombic efficiencies, (ii) voltage profiles, and (iii) corresponding differential capacity curves for Ge nanowire batteries cycled galvanostatically using an electrolyte solution of 1.0 M $LiPF_6$ dissolved in 1:1 w/w mixtures of (a) EC:DEC, (b) EC:DMC, (c) EC:DMC + 3% w/w FEC, (d) FEC:DEC, (e) FEC:DMC.

(ratio of discharge to charge capacity at each cycle), voltage profiles and differential capacity plots for the battery tests in Figure 3. The electrochemical data for PC:DMC electrolyte was not included in Figure 4 because of its poor cycle stability. The Coulombic efficiencies after the first few cycles were greater than 95% for all of the batteries in Figure 3, even those with the more significant capacity fade. The observed increase in Coulombic efficiency during the first few initial cycles is most likely related to SEI layer formation, but requires further study. Commercial applications require high Coulombic efficiencies—ideally close to 100%, as even a 99% Coulombic efficiency translates to 63% irreversible loss after 100 cycles—making this an important consideration in battery performance.

Differential capacity plots provide detailed information about the electrochemical processes in the battery and their stability. During the first cycle, the differential capacity plots (Figure 5) show a sharp lithiation peak near 350 mV with a smaller, yet still reasonably sharp peak at 150−200 mV. The sharp peak at

dx.doi.org/10.1021/am3010253 | ACS Appl. Mater. Interfaces 2012, 4, 4658−4664

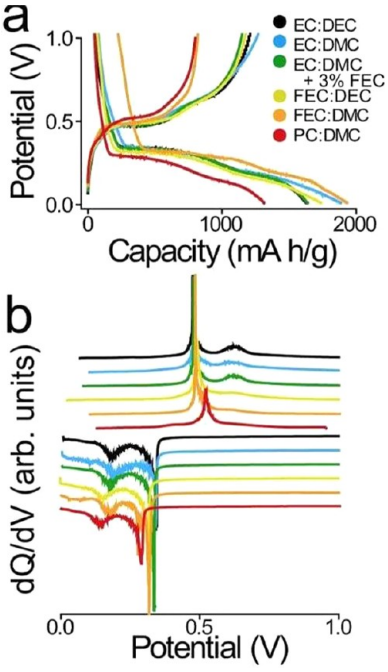

Figure 5. First cycle (a) voltage profiles and (b) differential capacity plots for Ge nanowires anodes with PVdF binder, conductive carbon and 1.0 M $LiPF_6$ in various electrolyte solvents.

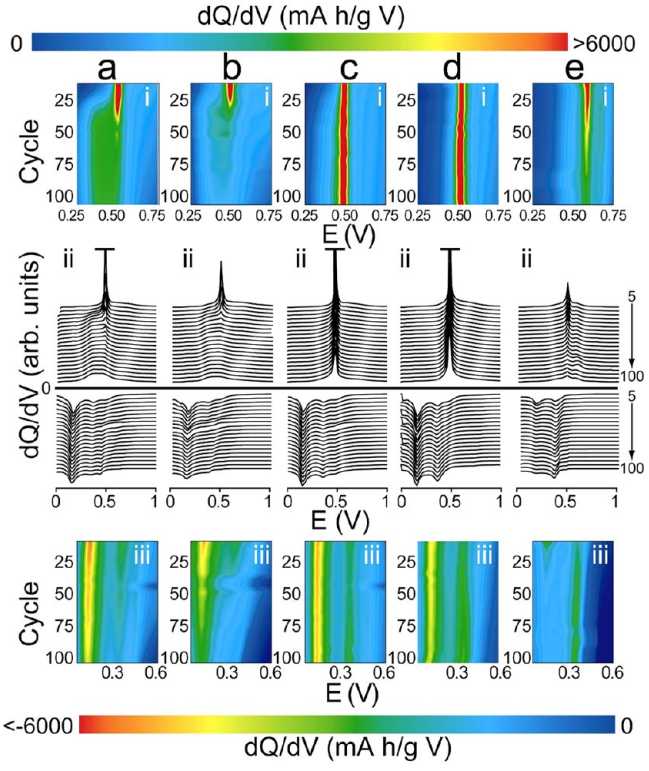

Figure 6. Differential capacity (i, iii) color maps and (ii) waterfall plots for Ge nanowire batteries with PVdF and conductive carbon (7:1:2 w/w/w Ge:C:PVdF) cycled from 0.01 to 2 V vs Li/Li^+ against Li foil with 1 M $LiPF_6$ in a 1:1 mixtures of electrolyte solvent: (a) EC:DEC, (b) EC:DMC, (c) EC:DMC + 3% FEC, (d) FEC:DEC, and (e) FEC:DMC. The differential capacity during discharge or delithiation is shown in the top two rows of data and charge or lithiation is shown in the bottom two rows.

350 mV corresponds to the lithiation of crystalline Ge.[10] Lithiation amorphizes Ge and this sharp lithiation peak no longer

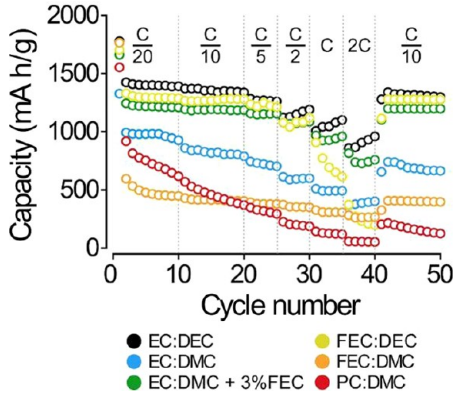

Figure 7. Charge (lithiation) capacity of Ge nanowire anodes with various electrolyte solvents cycled at different rates.

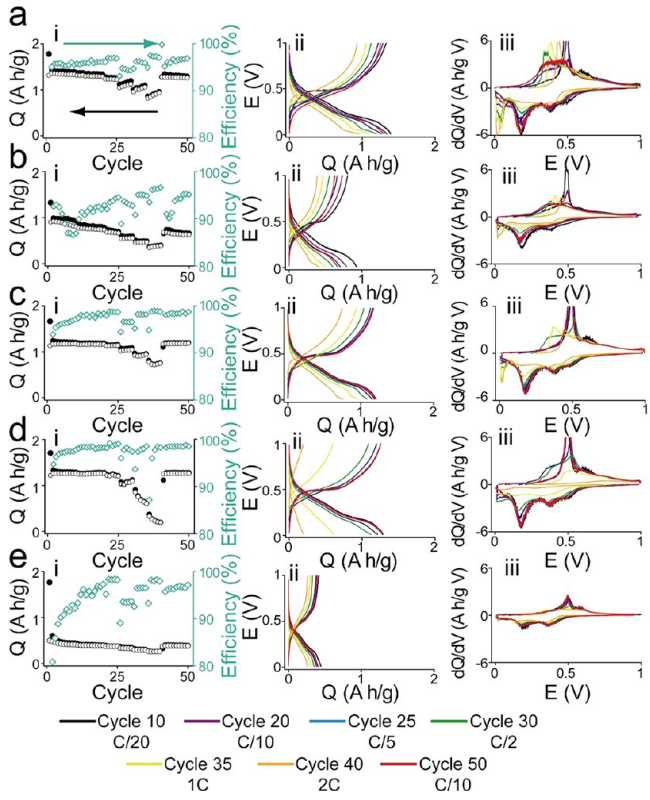

Figure 8. (i) Charge (lithiation) and discharge (delithiation) capacity (Q), Coulombic efficiency, (ii) voltage profiles, and (iii) differential capacity of Ge nanowire anodes at different cycle rates and electrolyte (1 M $LiPF_6$): (a) EC:DEC, (b) EC:DMC, (c) EC:DMC + 3% FEC, (d) FEC:DEC, and (e) FEC:DMC.

appears in subsequent cycles. Instead, lithiation produces three relatively broad lithiation peaks at 500, 350, and 200 mV, characteristic of lithiation of amorphous Ge (a-Ge).[38]

Delithiation gives rise to a very prominent sharp peak at 500 mV, which is consistent with other reports for Ge delithiation.[10,12,15,18,21,38,39] On the first delithiation cycle (Figure 5), this sharp peak is also accompanied by a lower intensity, broad peak at 600 mV. At later cycles in the more stable batteries, this 600 mV peak is still present but with very weak intensity. One of the clearest signatures of capacity fade was the disappearance of the sharp delithiation peak at 500 mV. This is more clearly viewed in waterfall plots (Figure 6). The batteries with EC:DEC and EC:DMC electrolyte that had significant capacity fade

dx.doi.org/10.1021/am3010253 | ACS Appl. Mater. Interfaces 2012, 4, 4658−4664

lost the sharp delithiation peak at later cycles, which was replaced by a broad, less intense delithiation peak at lower voltage at about 400 mV. In Si anodes, there is a sharp delithiation peak in the differential capacity corresponding to the delithiation of crystalline $Li_{15}Si_4$.[40] Delithiation of amorphous Li_xSi produces broader peaks.[40] The sharp delithiation peak observed for the most stable Ge nanowire anodes might indicate that the highest capacities are achieved when Ge is fully lithiated reversibly to crystalline $Li_{15}Ge_4$.

Rate Capability. The rate capability of Ge nanowire anodes was also tested. Figure 7 shows capacity data for batteries made with various electrolyte solvents cycled at different rates. EC:DMC+3% FEC electrolyte again gave the best performance. Batteries with EC:DEC electrolyte also exhibited good performance, with high capacity even at faster cycle rates. But the batteries were only cycled ten times at each rate and the EC:DEC batteries had significant drift, indicating relative instability. The EC:DMC+3%FEC containing batteries exhibited high capacity of about 700 mA h g^{-1} at 2*C* without similar drift. The FEC:DEC containing battery also performed very well at the slow cycle rates, but the capacity dropped sharply once the rate exceeded *C*/2.

Figures 8 and 9 show the voltage profiles and differential capacity plots that correspond to the battery data in Figure 7.

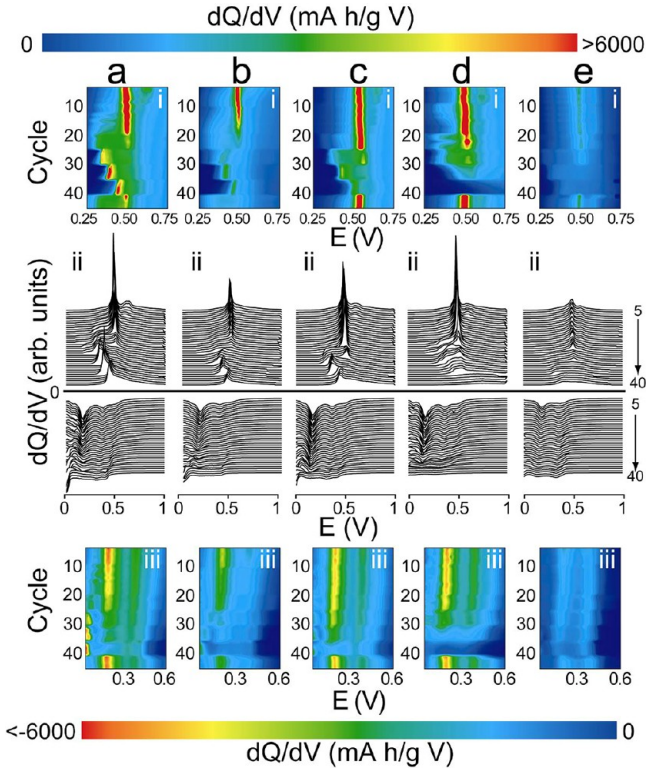

Figure 9. Differential capacity (i,iii) color maps and (ii) waterfall plots for Ge nanowire batteries cycled at various cycle rate and different electrolyte (1 M $LiPF_6$) solvents, (a) EC:DEC, (b) EC:DMC, (c) EC:DMC + 3% FEC, (d) FEC:DEC, and (e) FEC:DMC.

When cycle rate was increased above *C*/5 and the capacity dropped, the sharp delithiation peak at 500 mV decreased significantly in intensity and shifted to lower potential. This distinct shift in the delithiation peak to lower potential might indicate a slightly altered delithiation pathway at the faster cycle rates. As the rate was further increased above *C*/2, the delithiation peak shifted back toward 500 mV. The shift in the

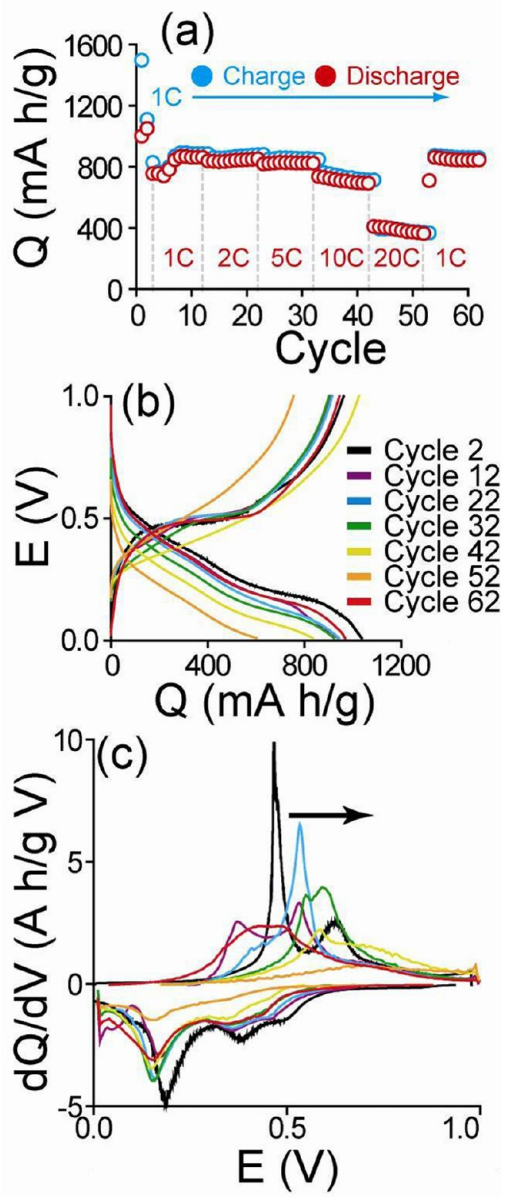

Figure 10. (a) Charge (lithiation) and discharge (delithiation) capacity *Q*, for a Ge nanowire anode with PVdF binder and 1.0 M $LiPF_6$ in EC:DMC+3%FEC charged at a rate of 1*C* and discharged at various rates. (b, c) Voltage profiles and differential capacity curves corresponding to the cycle data in (a).

delithiation peak to higher potential and the lithiation peaks to lower potential with faster cycle rates indicate that the kinetic limitations are limiting the capacity of the battery. These changes were reversible for the FEC-containing batteries when the cycle rate returned to *C*/10. The lithiation and delithiation features, especially the sharp delithiation peak at 500 mV, in the batteries with significant capacity fade, i.e., those with EC:DEC and EC:DMC electrolyte, did not return when the cycle rate returned to *C*/10.

Ge is known to perform very well at high cycle rates;[7,8,10] however, the data in Figure 7 showed that the capacity of the Ge nanowire anodes suffered when the rate exceeded *1C*. For many applications, the charging and discharging rates do not need to be equivalent. For example, an electrical vehicle might tolerate a slower charge rate, but in certain situations like rapid acceleration need a fast burst of discharge. The Ge nanowire anodes were

dx.doi.org/10.1021/am3010253 | ACS Appl. Mater. Interfaces 2012, 4, 4658−4664

tested under a similar condition by charging at a relatively slow rate of 1*C*, but then discharging at faster rates. As shown in Figure 10, even with a very fast discharge at 10*C*, the capacity only dropped from 1050 to 900 mA h g^{-1}. These values are higher than a recent demonstration of Ge nanotubes cycled at fast rates (10C) with a reported capacity of 650 mA h g^{-1}.[8] A significant drop in capacity was only observed when the rate was increased from 10*C* to 20*C*. The 2400 Celgard separator membrane becomes limiting at very fast rates and could explain the significant drop in capacity here when the discharge rate was increased from 10*C* to 20*C*. Other membranes that might perform better at higher cycle rates with Ge anodes are under investigation.[41] These data indicate that Ge is a good candidate for applications requiring high power during discharge.

Long-Term Cycle Stability. The electrolyte solvents EC:DMC+3%FEC and FEC:DEC yielded the best performance with very little capacity fade after 100 cycles at a rate of *C*/10. To determine the limits of their long-term stability, these batteries were further tested with the faster cycling rate of 1*C* as shown in Figure 11. The increased cycle rate led to a drop in capacity.

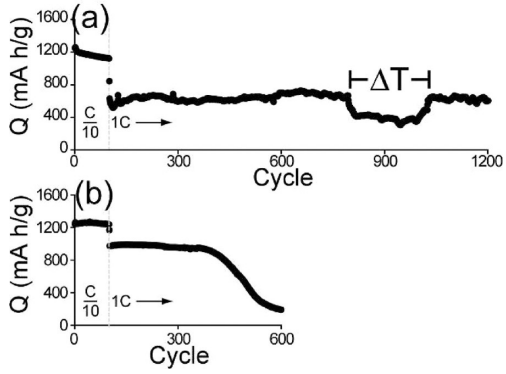

Figure 11. Long term cycle stability of Ge nanowire anodes with (a) EC:DMC+3%FEC and (b) FEC:DEC electrolyte. In (a), the span in data labeled with ΔT were acquired when the lab temperature was decreased from 75 °F (24 °C) to 60 °F (16 °C). The first 100 cycles at a rate of *C*/10 are also shown.

After the change in cycle rate, the FEC:DEC battery had the higher capacity of just above 1000 mA h g^{-1}. The battery cycled reversibly for the first 300 cycles, but then faded significantly, with the capacity decreasing to near 200 mA h g^{-1} after the 600th cycle. The capacity of the battery with EC:DMC+3%FEC dropped from just above 1200 to 700 mA h g^{-1} initially when the cycle rate was increased to 1*C*, but retained this capacity even after 1200 cycles.

The data in Figure 11 also show that the battery response is sensitive to temperature. During most of the measurements, the lab temperature was 75°F (24°C), but was decreased for several days to 60°F (16°C) during cycles 750 and 1050 as indicated in Figure 9a. The decrease in ambient temperature reduced the capacity significantly to 400 mA h g^{-1}. When the temperature returned to 75°F, the capacity also returned to almost 700 mA h g^{-1}.

CONCLUSIONS

Ge nanowire Li-ion battery anodes were tested with PVdF binder and a variety of electrolyte solutions. Similar to Si-based anodes,[25] FEC provided a stabilizing effect for the Ge nanowire anodes. The Ge nanowires exhibited stable and high capacity of 1,248 mA h g^{-1} close to the theoretical capacity of Ge. This corresponds approximately to a volumetric capacity of 920 A h L^{-1}, which is just above the theoretical volumetric capacity of graphite (830 A h L^{-1}).[3,42] The Ge nanowire anodes also performed well at fast cycle rates, indicating that Ge nanowires might be suitable for very high power density and high rate applications.

AUTHOR INFORMATION

Corresponding Author

*E-mail: korgel@che.utexas.edu. Phone: 1-512-471-5633. Fax: 1-512-471-7060.

Notes

The authors declare no competing financial interest.

ACKNOWLEDGMENTS

We thank Tim Bogart, Justin Harris, Paul Abel, and Yong-Mao Lin for insightful discussions, TIMCAL for supplying carbon black, TCI America for supplying FEC, and Celgard for supplying separator membranes. Financial support of this research was provided in part by the Robert A. Welch Foundation (BAK grant F-1464 and CBM grant F-1436) and the Air Force Research Laboratory (FA-8650-07-2-5061). KCK acknowledges the NSF Graduate Research Fellowship program for financial support. The supply of Ge nanowires was supported as part of the program "Understanding Charge Separation and Transfer at Interfaces in Energy Materials (EFRC: CST)", an Energy Frontier Research Center by the U.S. Department of Energy, Office of Science, Office of Basic Energy Sciences, under Award DE-SC0001091.

REFERENCES

(1) Armand, M.; Tarascon, J. M. *Nature* **2008**, *451*, 652−657.
(2) Goodenough, J. B.; Kim, Y. *Chem. Mater.* **2009**, *22*, 587−603.
(3) Hayner, C. M.; Zhao, X.; Kung, H. H. *Annu. Rev. Chem. Biomol. Eng.* **2012**, *3*, 445−471.
(4) Winter, M.; Besenhard, J. O.; Spahr, M. E.; Novák, P. *Adv. Mater.* **1998**, *10*, 725−763.
(5) Liu, X. H.; Liu, Y.; Kushima, A.; Zhang, S.; Zhu, T.; Li, J.; Huang, J. Y. *Adv. Energy Mater.* **2012**, DOI: 10.1002/aenm.201200024.
(6) Fuller, C. S.; Severiens, J. C. *Phys. Rev.* **1954**, *96*, 21−24.
(7) Wang, J.; Du, N.; Zhang, H.; Yu, J.; Yang, D. *J. Mater. Chem.* **2011**, *22*, 1511−1515.
(8) Park, M.-H.; Cho, Y.; Kim, K.; Kim, J.; Liu, M.; Cho, J. *Angew. Chem., Int. Ed.* **2011**, *50*, 9647−9650.
(9) Baggetto, L.; Notten, P. H. L. *J. Electrochem. Soc.* **2009**, *156*, A169−A175.
(10) Graetz, J.; Ahn, C. C.; Yazami, R.; Fultz, B. *J. Electrochem. Soc.* **2004**, *151*, A698−A702.
(11) Hwang, C.-M.; Park, J.-W. *Thin Solid Films* **2010**, *518*, 6590−6597.
(12) Laforge, B.; Levan-Jodin, L.; Salot, R.; Billard, A. *J. Electrochem. Soc.* **2008**, *155*, A181−A188.
(13) Wang, D.; Yang, Z.; Li, F.; Liu, D.; Wang, X.; Yan, H.; He, D. *Mater. Lett.* **2011**, *65*, 1542−1544.
(14) Baggetto, L. C.; Hensen, E. J. M.; Notten, P. H. L. *Electrochim. Acta.* **2010**, *55*, 7074−7079.
(15) DiLeo, R. A.; Frisco, S.; Ganter, M. J.; Rogers, R. E.; Raffaelle, R. P.; Landi, B. J. *J. Phys. Chem. C* **2011**, *115*, 22609−22614.
(16) Cheng, J.; Du, J. *CrystEngComm* **2012**, *14*, 397−400.
(17) Xue, D.-J.; Xin, S.; Yan, Y.; Jiang, K.-C.; Yin, Y.-X.; Guo, Y.-G.; Wan, L.-J. *J. Am. Chem. Soc.* **2012**, *134*, 2512−2515.
(18) Seo, M.-H.; Park, M.; Lee, K. T.; Kim, K.; Kim, J.; Cho, J. *Energy Environ. Sci.* **2011**, *4*, 425−428.
(19) Liu, X. H.; Huang, S.; Picraux, S. T.; Li, J.; Zhu, T.; Huang, J. Y. *Nano Lett.* **2011**, *11*, 3991−3997.
(20) Ko, Y. D.; Kang, J. G.; Lee, G. H.; Park, J. G.; Park, K. S.; Jin, Y. H.; Kim, D. W. *Nanoscale* **2011**, *3*, 3371−3375.
(21) Chan, C. K.; Zhang, X. F.; Cui, Y. *Nano Lett.* **2007**, *8*, 307−309.

(22) Chockla, A. M.; Panthani, M. G.; Holmberg, V. C.; Hessel, C. M.; Reid, D. K.; Bogart, T. D.; Harris, J. T.; Mullins, C. B.; Korgel, B. A. *J. Phys. Chem. C* **2012**, *16*, 11917−11923.
(23) Chockla, A. M.; Korgel, B. A. *J. Mater. Chem.* **2009**, *19*, 996−1001.
(24) Saunders, A. E.; Sigman, M. B.; Korgel, B. A. *J. Phys. Chem. B* **2003**, *108*, 193−199.
(25) Chockla, A. M.; Bogart, T. D.; Hessel, C. M.; Klavetter, K.; Mullins, C. B.; Korgel, B. A. *J. Phys. Chem. C* **2012**, DOI: 10.1021/jp305371v.
(26) Chockla, A. M.; Harris, J. T.; Akhavan, V. A.; Bogart, T. D.; Holmberg, V. C.; Steinhagen, C.; Mullins, C. B.; Stevenson, K. J.; Korgel, B. A. *J. Am. Chem. Soc.* **2011**, *133*, 20914−20921.
(27) Chan, C. K.; Patel, R. N.; O'Connell, M. J.; Korgel, B. A.; Cui, Y. *ACS Nano* **2010**, *4*, 1443−1450.
(28) Etacheri, V.; Haik, O.; Goffer, Y.; Roberts, G. A.; Stefan, I. C.; Fasching, R.; Aurbach, D. *Langmuir* **2011**, *8*, 965−976.
(29) Choi, N.-S.; Yew, K. H.; Lee, K. Y.; Sung, M.; Kim, H.; Kim, S.-S. *J. Power Sources* **2006**, *161*, 1254−1259.
(30) Nakai, H.; Kubota, T.; Kita, A.; Kawashima, A. *J. Electrochem. Soc.* **2011**, *158*, A798−A801.
(31) Lin, Y.-M.; Klavetter, K. C.; Abel, P. R.; Davy, N. C.; Snider, J. L.; Heller, A.; Mullins, C. B. *Chem. Commun.* **2012**, *48*, 7268−7270.
(32) Li, J.; Christensen, L.; Obrovac, M. N.; Hewitt, K. C.; Dahn, J. R. *J. Electrochem. Soc.* **2008**, *155*, A234−A238.
(33) Chen, Z.; Christensen, L.; Dahn, J. R. *Electrochem. Commun.* **2003**, *5*, 919−923.
(34) Kovalenko, I.; Zdyrko, B.; Magasinski, A.; Hertzberg, B.; Milicev, Z.; Burtovyy, R.; Luzinov, I.; Yushin, G. *Science* **2011**, *334*, 75−79.
(35) Mazouzi, D.; Lestriez, B.; Roue, L.; Guyomard, D. *Electrochem. Solid St.* **2009**, *12*, A215−A218.
(36) Magasinski, A.; Zdyrko, B.; Kovalenko, I.; Hertzberg, B.; Burtovyy, R.; Huebner, C. F.; Fuller, T. F.; Luzinov, I.; Yushin, G. *ACS Appl. Mater. Interfaces* **2010**, *2*, 3004−3010.
(37) Bridel, J. S.; Azaïs, T.; Morcrette, M.; Tarascon, J. M.; Larcher, D. *Chem. Mater.* **2009**, *22*, 1229−1241.
(38) Yoon, S.; Park, C.-M.; Sohn, H.-J. *Electrochem. Solid-State Lett.* **2008**, *11*, A42−A45.
(39) Lee, H.; Kim, H.; Doo, S.-G.; Cho, J. *J. Electrochem. Soc.* **2007**, *154*, A343−A346.
(40) Obrovac, M. N.; Krause, L. J. *J. Electrochem. Soc.* **2007**, *154*, A103−A108.
(41) Djiana, D.; Alloinb, F.; Martineta, S.; Ligniera, H.; Sanchez, J. Y. *J. Power Sources* **2007**, *172*, 416−421.
(42) The volumetric capacity is estimated based on the measured specific capacity of 1250 mA h g^{-1}, the density of 7:2:1 w/w/w Ge/binder/conductive carbon material loaded onto the current collector (1 mg cm^{-2}), and the 10 μm thick electrode thickness.